To be submitted to ApJL

Interacting Coronal Mass Ejections and Solar Energetic Particles

N. Gopalswamy[1], S. Yashiro[1,2], G. Michałek[1,2], M. L. Kaiser[2], R. A. Howard[3], D. V. Reames[2], R. Leske[4], and T. Von Rosenvinge[2]

ABSTRACT

We studied the association between solar energetic particle (SEP) events and coronal mass ejections (CMEs) and found that CME interaction is an important aspect of SEP production. Each SEP event was associated with a primary CME that is faster and wider than average CMEs and originated from west of E45. For most of the SEP events, the primary CME overtakes one or more slower CMEs within a heliocentric distance of ~ 20 $R_\odot$. In an inverse study, we found that for all the fast (speed > 900 km s^{-1}) and wide (width > 60 deg) western hemispheric frontside CMEs during the study period, the SEP-associated CMEs were ~ 4 times more likely to be preceded by CME interaction than the SEP-poor CMEs. i.e., CME interaction is a good discriminator between SEP-poor and SEP-associated CMEs. We infer that the efficiency of the CME-driven shocks is enhanced as they propagate through the preceding CMEs and that they accelerate SEPs from the material of the preceding CMEs rather than from the quiet solar wind. We also found a high degree of association between major SEP events and interplanetary type II radio bursts suggesting that proton accelerators are also good electron accelerators.

Subject headings: Sun: coronal mass ejections (CMEs)– Sun: radio radiation – Sun: particle emission - Sun: corona - Sun: solar-terrestrial relations

[1]Code 695, NASA/GSFC, Greenbelt, MD 20771

[2]Center for Solar Physics and Space Weather, The Catholic University of America, Washington DC 20064

[3]Naval Research Laboratory, Washington, DC

[4]California Institute of Technology, Mail Code 220-47, Pasadena, CA 91125

1. Introduction

Large solar energetic particles (SEPs) events are known to be closely related to coronal mass ejections (CMEs) (see, e.g., Reames 1999). Fast CMEs drive MHD shocks, which in turn accelerate the SEPs (protons and minor ions). SEP acceleration may also occur during flares, but these events are typically short-lived (hours). For space weather purposes, the large gradual SEPs from CME-driven shocks are more important. More than 4500 CMEs were observed from January 1996 to the end of 2001 (see the CME catalog in http://cdaw.gsfc.nasa.gov/), yet only ∼100 SEP events with I_p (intensity of > 10 MeV protons) exceeding 1 pfu (= 1 proton $cm^{-2}s^{-1}sr^{-1}$) were observed during the same period. Thus only a small fraction (1-2%) of CMEs is associated with SEPs and it is important to know what makes a CME an SEP accelerator. It is known that the CME speed and the SEP intensity are well correlated (Kahler 2001). Faster and wider CMEs produce decameter-hectometric (DH) type II radio bursts so they must be good electron accelerators (Gopalswamy et al. 2001a). Recently, Gopalswamy et al. (2001b, 2002) found that interaction between CMEs can influence the production of nonthermal electrons, as inferred from intense radio emission in the interplanetary (IP) medium. In this paper, we investigate whether CME interactions are also important for SEP production.

2. Data Selection and Analysis

From GOES proton data we identified 43 major ($I_p \geq 10$ pfu) and 39 minor (1 pfu $\leq I_p < 10$ pfu) SEP events from January 1996 to November 4, 2001 by requiring that simultaneous data exist for SEPs and CMEs. The CMEs were observed by the Solar and Heliospheric Observatory (SOHO) mission's Large Angle and Spectrometric Coronagraphs (LASCO, Brueckner et al. 1995) known as C2 and C3. Each SEP event corresponds to a unique white-light CME, which we call the primary CME as listed in Table 1. In addition to the SEP date (column 1) and onset time (column 2), the CME onset (column 3), speed (V in column 4), width (W in column 5), and the heliographic coordinates of the solar sources (column 6) are also listed. The solar sources were obtained from the on-line Solar Geophysical Data (SGD) as the location of the associated Hα flare. When Hα information is not available, we used movies from the Extreme-ultraviolet Imaging Telescope (EIT) on board SOHO and the Yohkoh mission's soft X-ray telescope to identify the location of the eruption. For one major event (01/08/09) we identified the location of the eruption (S17E19) from EIT images, but the CME could not be measured. For some events the solar sources were behind the west limb (noted as backside or (b) in column 6). Whether or not an SEP event was associated with a type II burst in the metric (y for yes and n for no) and DH (Y

for yes and N for no) wavelengths is noted in column 7. Information on the metric type II bursts were obtained from SGD. The DH type II bursts were observed by the Radio and Plasma Wave Experiment (WAVES, Bougeret et al. 1995) on board the Wind spacecraft.

Height-time plots of CMEs were extended to 30 and 50 $R_\odot$ to see if the trajectories of the preceding CMEs intersect that of the primary CME. We also required that the preceding CMEs with intersecting trajectories have a position angle (PA) overlap (Δw) with the primary CMEs. When $\Delta w > 30^\circ$ we designated the interaction to be full (F) and partial (P) when $\Delta w < 30^\circ$. We also played movies of LASCO images to visually examine and confirm the physical overlap. Events with height-time overlap, but no PA overlap were eliminated. The extent of CME interaction is listed in column 8 (Int) of Table 1: F and P are suffixed by the number of CMEs interacting with the primary CME. When the intersection of trajectories occur between 30 and 50 $R_\odot$, we added a question mark to indicate that the interaction may be less severe. Some events had both F and P interactions (marked by an asterisk in columns 8 and 16). In a few cases, there was no obvious interaction with a preceding CME, but there was clear interaction with one of the legs of a preceding CME (marked as NL) or with a bright western streamer (marked as NS). NH denotes interaction with a preceding halo. Events with no obvious interaction with any of these features are marked by N (including purely eastern interactions). Two examples of the height-time plots are shown in Figure 1: the November 6, 1997 event is preceded by an F1 interaction, while the October 1, 2001 event is preceded by an F4 interaction. We have used linear fits to the height-time plots in determining the height of intersection between the primary and preceding CMEs. If we use quadratic fits, we expect a slightly larger number of interactions. Columns 9-16 of Table 1 have all the information for the minor SEP events. In the next section we describe the results of our analysis.

3. Results

3.1. Characteristics of the Primary CMEs

The primary CMEs of the major SEPs were the fastest (average speed $\sim$1393 km s^{-1}, see Fig. 2a), while those of the minor SEPs were slightly slower (average speed $\sim$927 km s^{-1}, see Fig. 2b). All the primary CMEs had speeds exceeding the average speed ($\sim$ 450 km s^{-1}) of the general population of CMEs. The longitude distribution of the solar sources of the primary CMEs is similar for the major and minor SEPs (Fig. 2(c-d)). All the solar sources were west of E46. The last bin (90+) in Fig. 2(c-d) containing the behind-the-limb events, is the largest for both sets of SEPs. The longitude distribution is also somewhat different from the canonical distribution of gradual SEP events (Reames 1995), which extended all

the way to the east limb. Table 1 (columns 5 and 13) shows that a major fraction of the primary CMEs were halos. In fact, the primary CMEs of 98% of the major SEPs and 87% of the minor SEPs had widths exceeding 100° (see Table 2). Although we cannot measure the actual widths of halo CMEs, we can say that the SEP accelerators expand rapidly to acquire a large angular size within the coronagraph field of view. Thus, the SEP-associated primary CMEs are very fast and very wide and occur west of E45.

3.2. SEPs and CME Interaction

Table 1 shows that a vast majority of the primary CMEs (35/42 or 83% for major SEPs and 33/39 or 84% for minor SEPs) interacted with one or more preceding CMEs. These percentages go up to 93% and 95% for major and minor events, respectively when NH, NL, and NS interactions are included. Single interactions were most common, but there were also some multiple interactions. The preceding CMEs were mostly slow events (average speeds of 436 and 356 km s^{-1} for major and minor events, respectively; see Fig. 2(e-f)). The PA overlap (Δw) between the primary and the preceding CMEs is typically $\sim$50° (Fig. 2(g-h)). The preceding CMEs that interact with the primary CMEs depart typically a few hours earlier (average $\sim$ 7 hr, see Fig. 2(i-j)). The heliocentric distance at which the leading edges of the primary and preceding CMEs intersect is $\sim$ 21 $R_\odot$ (Fig. 2(k-l)). Since CMEs have a finite thickness, the interaction must start much before the intersection of leading-edge trajectories. From the radio emission characteristics of interacting CMEs, Gopalswamy et al. (2001b) found that the interaction starts $\sim$1 hr before the intersection of trajectories. Furthermore, when the height-time measurements are made at the PA of interaction rather than that of fastest motion in the CMEs (as was done here), the trajectories would intersect at lower heights.

3.3. Inverse Study of Fast and Wide CMEs and SEPs

One might wonder if the above result is simply due to the fact that CMEs are more frequent during solar maximum, so CME interaction must be commonplace. To show that this is not the case, we examined the CME interaction and SEP association for all the fast (speed > 900 km s^{-1}) and wide (width $> 60°$) CMEs with a westward bias (halos and western-hemisphere events) that occurred during the study period. We also required that the CME span must include PA 270° to increase the likelihood of involving the Sun-Earth flux tube. There were 124 such CMEs, but many of them originated from behind the limb. The SEP association was not clear for some events due to the enhanced SEP background from previous

events, which we dropped. In order to develop a clean sample, we considered only the front side, western hemisphere CMEs. This resulted in 52 fast and wide (F/W) CMEs of which 42 were associated with SEPs (above the GOES threshold and unambiguously distinguishable as a separate event when the background is high) and the remaining 10 (19%) were not (see Table 2). Table 3 summarizes the SEP association and the extent of CME interaction for these CMEs. The numbers under the 'Minor SEP' column include a few weaker events with $I_p < 1$ pfu, but above GOES threshold; $I_p \geq 1$ pfu minor events are shown within parentheses. Interactions in the eastern hemisphere are unlikely to be relevant for SEP events, so we included four such events in the 'No interaction' category. We see that the number of SEP-poor CMEs with (6/10) and without (4/10) CME interaction is roughly the same. On the other hand, 35/42 (= 83%) of SEP-associated CMEs interacted with preceding CMEs, while only 7/42 (= 17%) did not. Considering just the full interactions, we see that only 2/10 (= 20%) of SEP-poor CMEs were preceded by CME interaction compared to 33/42 (= 79%) for SEP-associated CMEs. We note that the SEP-poor CMEs had an average speed of 1220 km s^{-1}, significantly higher than that of the minor-SEP CMEs and close to that of major-SEP CMEs in Table 1, with a similar comparison for SEP-associated F/W CMEs. Five of the SEP-poor CMEs were halos and 8/10 (= 80%) had widths $> 100°$. Thus the CME interaction seems to discriminate the SEP-poor and SEP-associated ones since the speed and width of the two populations are comparable.

3.4. Type II Radio Bursts and SEPs

All but two (40/42 = 95%) of the major SEP events were associated with DH type II bursts (see Table 1, columns 7 and 15). The DH type II bursts are known to be associated with faster and wider (hence more energetic) CMEs (Gopalswamy et al. 2001a). Shocks driven by these CMEs accelerate electrons, which in turn produce the radio bursts. The high degree of association between major SEP events and DH type II bursts suggests that the proton accelerators are also good electron accelerators. The association is somewhat poorer for the minor SEP events: only 22/39 or 56% of the minor SEP events were associated with DH type II bursts. The metric type II burst association is poorer for both major (71%) and minor (59%) SEP events. The poor association between metric type II bursts and SEP events resembles a similar relationship between metric type II bursts and interplanetary shocks (Gopalswamy et al. 2001c). The type II radio burst association seems to be the only property that is significantly different for the major and minor SEP events. Interestingly, none of the SEP-poor F/W CMEs (see section 3.3) were associated with DH type II bursts.

4. Discussion and Conclusions

The primary results of this paper is that a major fraction of the SEP events occur at times of CME interaction. Each SEP event is associated with a primary CME, which sweeps up one or more slower CMEs in the near-Sun interplanetary medium. The estimated height of intersection close to the Sun ($\sim$ 20 $R_\odot$) is significant because SEPs are thought to be released when the associated CME reaches a height of $\sim$ 5-15 $R_\odot$ (Kahler 1994). The westward bias of the solar sources is consistent with the possibility that the Sun-Earth flux tube which carries SEPs is likely to be affected by the CME interaction. Furthermore the huge angular widths of the SEP producers ensures that they intersect the ecliptic. Using a sample of fast and wide front side CMEs, we were able to show that while the speeds, widths, and source locations of CMEs are important for predicting SEP events, the interaction with preceding CMEs proves to be another powerful discriminator.

The results presented in this paper have important implications to the theories of particle acceleration by shocks. The outermost structure of a fast CMEs is an MHD shock, which will first interact with the preceding CME. The shock has to pass through the inhomogeneous multithermal plasma (core, cavity and frontal of the preceding CMEs). Thus the shock has to accelerate the SEPs from the solar wind "contaminated" by the preceding CMEs, rather than from the quiet solar wind. Based on this, we suggest that the charge state composition of SEPs should rarely reflect the quiet solar wind conditions and that CME interaction may result in time-dependent, mixed impulsive-gradual signatures in SEP events. Mason et al. (1999) have attributed the mixed signatures to the 'lingering flare superthermals' in the in-ecliptic interplanetary medium.

The interaction rather than the speed of the preceding CMEs seems to be important for the SEP production. This argues against the pre-acceleration of the seed particles except in a few cases where the preceding CME also drives a shock. The interaction seems to enhance the acceleration efficiency of the shock either due to the higher density material (of the preceding CMEs) injected into the shock or due to the trapping of particles in the closed loops of the preceding CMEs. Passage of shocks through extremely dense streamers located nearby may also have similar effects.

This research was supported by AFOSR and NASA's SR&T, ISTP, and LWS programs. We thank the referee for many helpful comments. SOHO is a project of international cooperation between ESA and NASA.

REFERENCES

Bougeret, J.-L. et al. 1995, Space Sci. Rev., 71, 231

Brueckner, G. E. et al. 1995, Sol. Phys., 162, 357

Gopalswamy, N., Yashiro, S., Kaiser, M. L., Howard, R. A., & Bougeret, J.-L. 2001a, J. Geophys. Res., 106 , 29219

Gopalswamy, N. Yashiro, S., Kaiser, M. L., Howard, R. A., & Bougeret, J.-L. 2001b, ApJ, 548, L91

Gopalswamy, N., Lara, A., Kaiser, M. L., & Bougeret, J.-L. 2001c, J. Geophys. Res., 106, 25261

Gopalswamy, N., Yashiro, S., Kaiser, M. L., Howard, R. A., & Bougeret, J.-L. 2002 Geophys. Res. Lett., 29(8), 10.1029/2001GL013606.

Kahler, S. W. 1994, ApJ, 428, 837

Kahler, S. W. 2001, J. Geophys. Res., 106, 20947

Kahler, S. W. et al. 1984, J. Geophys. Res., 89, 9683

Mason, G. et al. 1999, ApJ, 525, L133

Reames, D. V. 1995, Rev. Geophys. Suppl., 33, 585

Reames, D. V. 1999, Space Sci. Rev., 90, 413

Table 1. Properties of primary CME associated with major and minor SEP events

MAJOR								MINOR							
SEP		CME						SEP		CME					
Date	Time	Time	V^a	W^b	Location	II[c]	Int[d]	Date	Time	Time	V^a	W^b	Location	II[c]	Int[d]
97/11/04	07:00	06:10	785	H	S14W33	yY	F1	97/04/07	12:00	14:27	878	H	S30E19	yY	F1
97/11/06	13:00	12:10	1556	H	S18W63	yY	F1	97/05/12	04:00	06:30	464	H	N21W08	yY	P1
98/04/20	11:00	10:07	1863	165	S43W90	yY	F1	97/11/13	23:00	22:25	546	288	NW90(b)	nN	F2
98/05/02	14:00	14:06	938	H	S15W15	yY	NH	97/11/14	14:00	13:36	702	217	N22W110	nN	NS
98/05/06	08:00	08:29	1099	190	S11W65	yY	F1*	98/04/30	00:00	16:58[p]	1374	H	S18E20	yY	F1*
98/05/09	05:00	03:35	2331	178	S11W90	yY	F1	98/06/04	09:00	02:04	1802	H	NW90(b)	nN	P3
99/04/24	15:00	13:31	1495	H	NW90(b)	nY	F2?	98/06/16	21:00	18:27	1484	281	S17W90	yY	F1?
99/05/03	13:00	06:06	1584	H	N15E32	yY	F3	99/05/09	19:00	18:27	615	172	N26W90	nN	F1
99/06/01	20:00	19:37	1772	H	NW90(b)	nY	F1	99/05/27	12:00	11:06	1691	H	NW90(b)	yY	NS
99/06/04	08:00	07:26	2230	150	N17W69	yY	F1?	99/06/11	01:00	01:26	719	101	SW90(b)	yN	F1?
00/02/18	10:00	09:54	890	118	S16W78	yY	F1?	00/01/18	19:00	17:54	739	H	S19E11	yY	F2
00/04/04	17:00	16:32	1188	H	N16W66	yY	F2	00/02/12	06:00	04:31	1107	H	N26W23	yY	F1*
00/06/06	19:00	15:54	1119	H	N20E18	yY	F3	00/02/17	22:00	20:06	600	H	S29E07	yY	F1*
00/06/10	18:00	17:08	1108	H	N22W38	yY	F4*	00/03/22	19:00	19:31	478	93	N14W57	yN	F1?
00/07/14	11:00	10:54	1674	H	N22W07	yY	F2	00/04/23	15:00	12:54	1187	H	N12W90	nN	N
00/07/22	12:00	11:54	1230	105	N14W56	yY	F1*	00/05/15	18:00	16:26	1212	165	S24W67	nY	F1
00/07/28	01:00	19:54[p]	905	H	Backside	nN	N	00/05/17	19:00	19:26	777	109	S22W37	nN	P1
00/08/11	12:00	07:31	1071	70	N27W90	nN	P1	00/06/17	03:00	03:28	857	133	N22W72	nY	F1?
00/09/12	13:00	11:54	1550	H	S17W09	yY	F1*	00/06/18	03:00	02:10	629	132	N23W85	yN	NL
00/10/16	08:00	07:27	1336	H	N05W90	yY	F3*	00/06/23	16:00	14:54	847	103	N26W72	yY	F1
00/10/25	12:00	08:26	770	H	N10W66	nY	F1?	00/06/25	10:00	07:54	1617	165	N16W55	yN	P1
00/11/08	23:00	23:06	1345	H	N10W77	nY	F2	00/07/11	14:00	13:27	1078	H	N18E27	nY	F2*
00/11/24	14:00	15:30	1245	H	N22W07	yY	F2*	00/07/12	19:00	20:30	820	101	N16W64	yY	F1
00/11/26	06:00	06:30	984	227	NW90(b)	nY	F1	00/08/13	06:00	06:06	883	154	NW90(b)	nN	F1
00/11/26	17:00	17:06	980	H	N18W38	yY	NL	00/09/19	14:00	08:50	766	76	N14W46	yY	F1*
01/01/28	17:00	15:54	916	250	S04W59	nY	N	00/11/04	03:30	01:50	763	100	S23W75	nN	F1
01/03/29	11:00	10:26	942	H	N20W19	yY	F1	00/11/24	06:00	05:30	994	H	N20W05	yY	F2
01/04/02	23:00	22:06	2505	244	N19W72	yY	F1?	00/12/28	16:00	12:06	930	H	Backside	nN	F2
01/04/10	08:00	05:30	2411	H	S23W09	yY	F2	01/01/05	19:00	17:06	828	H	SW90(b)	nN	F1*
01/04/12	12:00	10:31	1184	H	S19W43	yY	N	01/01/21	20:00	21:30[p]	1507	H	S07E46	yY	F1
01/04/15	14:00	14:06	1199	167	S20W85	yY	F3	01/02/11	03:00	01:31	1183	H	N24W57	yY	F3
01/04/18	03:00	02:30	2465	H	W120	yY	NS	01/02/26	08:00	05:30	851	152	NW90(b)	nY	NS
01/04/26	14:00	12:30	1006	H	N17W31	yY	F1?	01/03/25	15:00	17:06	677	H	N16E25	nN	P1?
01/05/07	13:00	12:06	1223	205	N25W35	nY	F2	01/04/02	12:00	11:26	992	80	N17W60	yY	F1
01/06/15	16:00	15:56	1701	H	SW90(b)	yY	F1	01/04/09	16:00	15:54	1192	H	S21W04	yY	N
01/08/09	19:00	...	...	...	S17E19	...	...	01/05/20	07:00	06:26	546	179	S16W90	yY	F2?
01/08/16	01:00	23:54[p]	1575	H	Backside	nY	P1	01/06/01	18:00	17:30	800	71	W90(b)	nN	F1
01/09/15	12:00	11:54	478	130	S21W49	yY	F1	01/06/04	17:00	16:30	464	89	N24W59	yN	F1?
01/09/24	11:00	10:30	2402	H	S16E23	nY	F1	01/10/19	02:00	01:27	558	254	N16W18	yY	P1?
01/10/01	13:00	05:30	1405	H	S20W90	nY	F4								
01/10/19	17:30	16:50	901	H	N15W29	yY	P1								
01/10/22	17:00	15:06	1336	H	S21E18	yY	F1								
01/11/04	17:00	16:35	1810	H	N06W18	yY	NS								

[a]Speed in km s^{-1}; [b]Width in degrees with H denoting full halos; [c]Type II Radio Burst; [d]Nature of interaction (N -no intercation; NH - interaction with a preceding halo CME; NL - interaction with one of the legs of a preceding CME; NS - interaction with one or more western bright streamers); [p]Previous day; *had also partial interaction

Table 2. Summary of Results

Property	Major SEP	Minor SEP
No. of Events	43	39
Average CME speed (km s^{-1})	1393	927
CME Longitude	> E32	> E46
Width > 100°	41/42 (98%)	34/39 (87%)
SEPs with CME Interaction	35/42 (83%)	33/39 (84%)
SEPs with All Interactions	39/42 (93%)	37/39 (95%)
Association with Metric Type II	30/42 (71%)	23/39 (59%)
Association with DH Type II	40/42 (95%)	22/39 (56%)
Interaction Time (Δt hr)	6.9	7.3
Height of intersection ($R_\odot$)	21	21
PA overlap (Δw deg)	50	53
F/W CMEs with SEPs	26/52	16/52
–Average CME speed (km s^{-1})	1433	1178
–Width > 100°	25/26 (96%)	15/16 (94%)

Table 3. Fast and Wide CMEs and SEPs

	No SEP	Minor SEP	Major SEP
No Interaction	4	3 (2)	4
Partial Interaction	4	1 (1)	1
Full Interaction	2	12 (7)	21

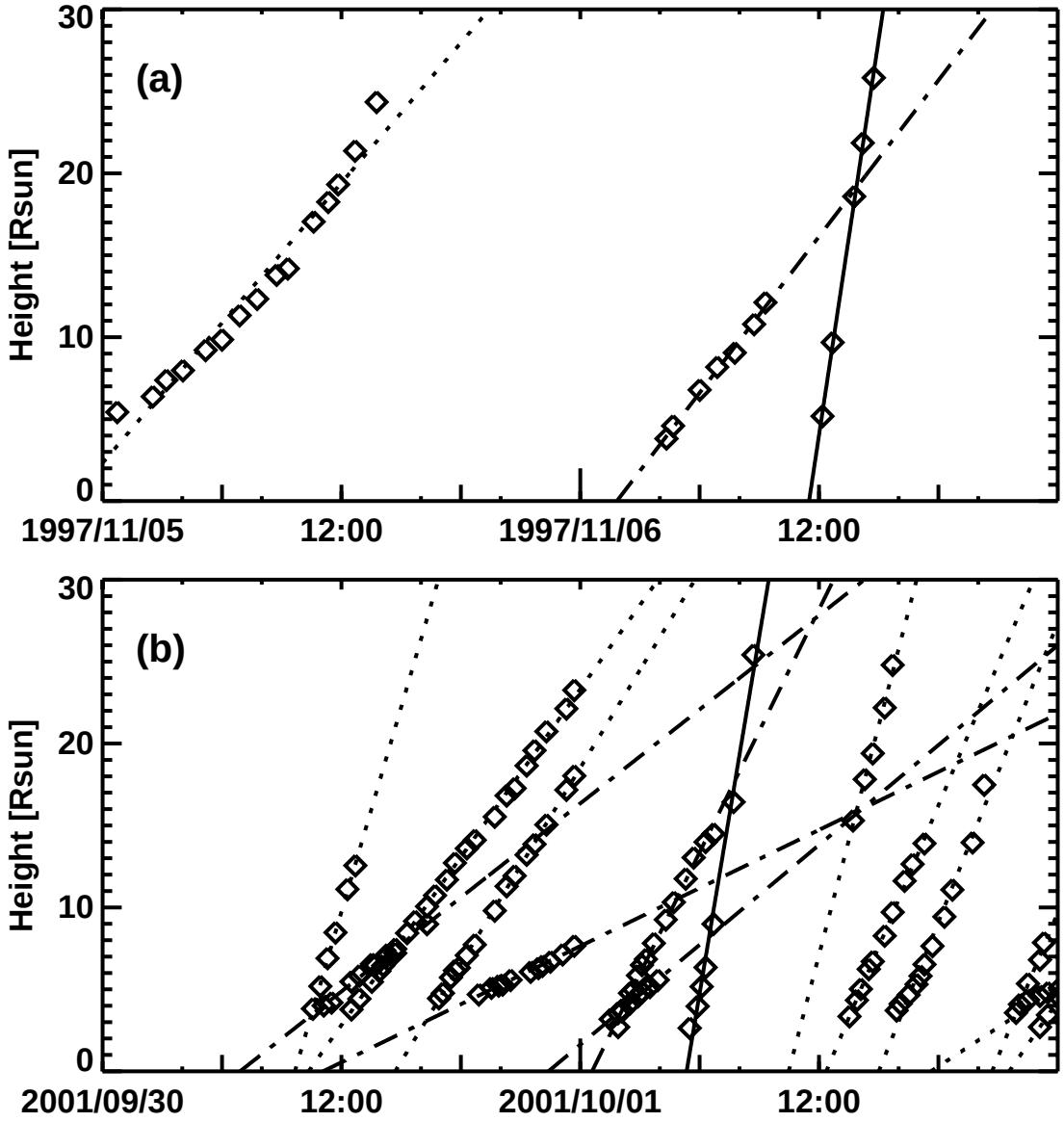

Fig. 1.— Height-time plots (diamonds: data points; lines: linear fits) of all the CMEs that preceded the primary CMEs (solid lines) within two days. CMEs interacting with the primary CMEs are shown by dot-dashed lines. Other CMEs occurring elsewhere and not interacting with the primary CMEs are shown by dotted lines. (a) The 1997 November 06 event with a single interaction (F1 in Table 1). (b) The 2001 October 1 event with multiple interactions (F4 in Table 1).

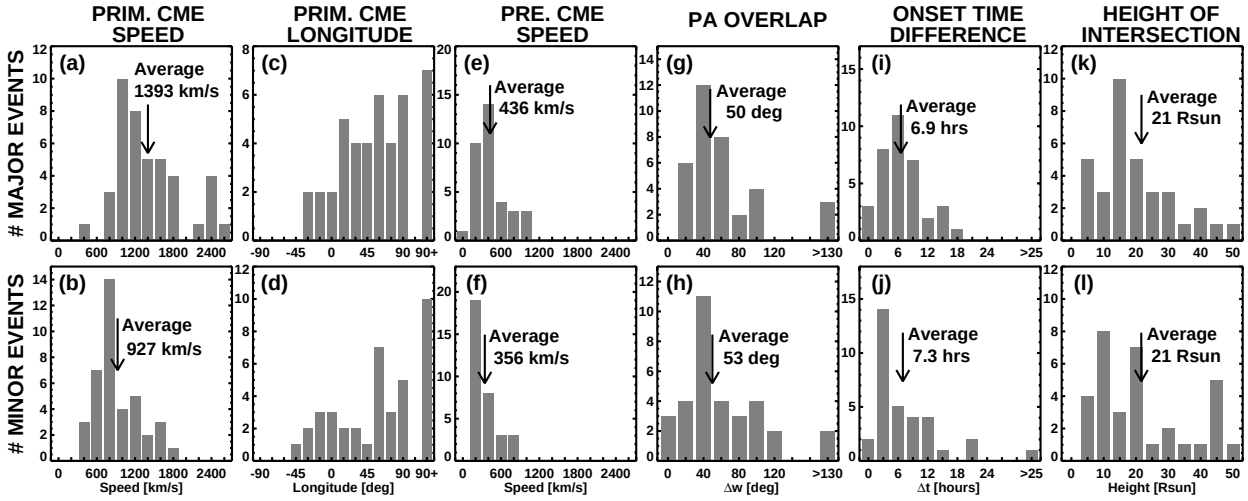

Fig. 2.— Properties of primary CMEs and interaction characteristics for major (top panel) and minor (bottom panel) SEP events. (a-b) Speeds and (c-d) source longitudes of primary CMEs; the last bin of longitude distribution (90+) contains all the backside CMEs. (e-f) Speed distribution of preceding CMEs that interact with the primaries. (g-h) Position angle overlap between the primary and preceding CMEs. (i-j) The time interval between the onsets of the primary and preceding CMEs. (k-l) The height at which the leading-edge trajectories of the primary and preceding CMEs intersect.